Structure, function, and ion-binding properties of a K^+ channel stabilized in the 2,4-ion–bound configuration

Cholpon Tilegenova[a,1], D. Marien Cortes[a,b], Nermina Jahovic[a,b], Emily Hardy[a,2], Parameswaran Hariharan[a,b], Lan Guan[a,b], and Luis G. Cuello[a,b,3]

[a]Cell Physiology and Molecular Biophysics, Texas Tech University Health Sciences Center, Lubbock, TX 79430; and [b]Center for Membrane Protein Research, Texas Tech University Health Sciences Center, Lubbock, TX 79430

Edited by Ramon Latorre, Centro Interdisciplinario de Neurociencias de Valparaíso, Facultad de Ciencias, Universidad de Valparaíso, Valparaíso, Chile, and approved July 10, 2019 (received for review February 1, 2019)

Here, we present the atomic resolution crystallographic structure, the function, and the ion-binding properties of the KcsA mutants, G77A and G77C, that stabilize the 2,4-ion–bound configuration (i.e., water, K^+, water, K^+-ion–bound configuration) of the K^+ channel's selectivity filter. A full functional and thermodynamic characterization of the G77A mutant revealed wild-type–like ion selectivity and apparent K^+-binding affinity, in addition to showing a lack of C-type inactivation gating and a marked reduction in its single-channel conductance. These structures validate, from a structural point of view, the notion that 2 isoenergetic ion-bound configurations coexist within a K^+ channel's selectivity filter, which fully agrees with the water–K^+-ion–coupled transport detected by streaming potential measurements.

ion permeation | KcsA | ion selectivity | potassium channels | selectivity filter

The K^+ channel's selectivity filter (SF) has captured the imagination of structural biologists for several decades. This overzealous scientific attention is based on its' role in catalyzing an unparalleled rapid and highly ion-selective transport. The molecular mechanism underlying this unique function has been the subject of functional, structural, and computational studies and yet remains a controversial topic of research (1–16).

K^+ channels are well-known for displaying permeability features that are compatible with a multiion conduction process. This hallmark functional characteristic was originally proposed based on the observation that the K^+ efflux from *Sepia* giant axons (under long-term voltage control) was inhibited by external K^+ ions. It was proposed then that the K^+ ions interact (also known as the "strict knock-on mechanism") while crossing the cell membrane and that they do so in a single-file fashion (17).

The SF of a K^+ channel consists of 4 consecutive ion-binding sites that were evidenced for the first time by macromolecular crystallography of the bacterial K^+ channel, KcsA (Fig. 1*A*) (18). Carbonyl groups from the peptide backbone of the signature sequence of K^+ channels (5) (*SI Appendix*, Fig. S1) (i.e., TTVGYGD), 2 from each subunit or 8 per channel-binding site (K^+ channels are tetramers), are perfectly arranged around each bound K^+ ion (Fig. 1*A*). In all available crystal structures of K^+ channels solved to date, a total of 4 K^+ ions have been observed in the SF (i.e., ion-binding sites S1, S2, S3, and S4, counting from the extracellular side) (Fig. 1*A*). This experimental observation in combination with electrostatic considerations form the basis of the canonical model for ion conduction in K^+ channels (16). It was proposed then that a K^+ channel's SF exists in 2 different isoenergetic arrangements known as the 1,3- and 2,4-ion–bound configurations (*SI Appendix*, Fig. S2). The interconversion of these SF configurations is driven by the electrostatic repulsion between K^+ ions separated by water molecules, a feature that underlies the rapid movement of ions within the channel's SF (*SI Appendix*, Fig. S3) (11, 15, 16).

Interestingly, a new model for ion conduction in K^+ channels, the so-called direct knock-on model, proposes that K^+ ions within the channel's SF can establish direct contact, triggering a very strong electrostatic repulsion, due to their very short interatomic distance, which propels the high transport rates exhibited by K^+ channels (*SI Appendix*, Fig. S4) (7, 19). However, a recent 2D infrared (2D IR) spectroscopic analysis suggested the presence of 2 ion-bound conformations in the SF (8), which was considered a settled proof in favor of the canonical model until it was recently challenged and shown that it can be explained by the direct knock-on mechanism (19).

Despite substantial experimental evidence and computational studies supporting these 2 different mechanistic proposals, a clear consensus is yet to be reached regarding the universality of a model for ion conduction in K^+ channels. As a result, this topic has reemerged as highly controversial (7–9, 19).

One of the strongest pieces of experimental evidence supporting the direct knock-on model was the calculation of the

Significance

Crystal structures of K^+ channels display 4 K^+ ions bound to the selectivity filter. Two mechanistic models have been proposed to explain this experimental observation. The "canonical model" proposes 2 alternating ion-bound configurations (1,3 and 2,4) coexisting within a channel's filter. Alternatively, in the "direct knock-on model" all binding sites are occupied at any given time, and ions establish direct contact. Here, it is shown the structure of a K^+-channel selectivity filter stabilized in the 2,4-ion configuration, which provides a definitive experimental demonstration for the canonical model of ion permeation in K^+ channels. In these structures, ions are separated by water molecules that seem to be cotransported during each ion transport cycle, which is in agreement with streaming potential measurements.

Author contributions: C.T., D.M.C., E.H., and L.G.C. designed research; C.T., D.M.C., N.J., E.H., and L.G.C. performed research; C.T., D.M.C., P.H., L.G., and L.G.C. contributed new reagents/analytic tools; P.H., L.G., and L.G.C. analyzed data; and L.G.C. wrote the paper.

The authors declare no conflict of interest.

This article is a PNAS Direct Submission.

Data deposition: Data have been deposited in the Protein Data Bank (accession numbers 6NFU [G77A], 6NFV [G77C], and 6PA0 [G77A in sodium]).

[1]Present address: Department of Antibody Engineering, Genentech, Inc., South San Francisco, CA 94080.

[2]Present address: Department of Cell Biology, University of Oklahoma Health Sciences Center, Oklahoma City, OK 73104.

[3]To whom correspondence may be addressed. Email: luis.cuello@ttuhsc.edu.

This article contains supporting information online at www.pnas.org/lookup/suppl/doi:10.1073/pnas.1901888116/-/DCSupplemental.

Published online August 6, 2019.

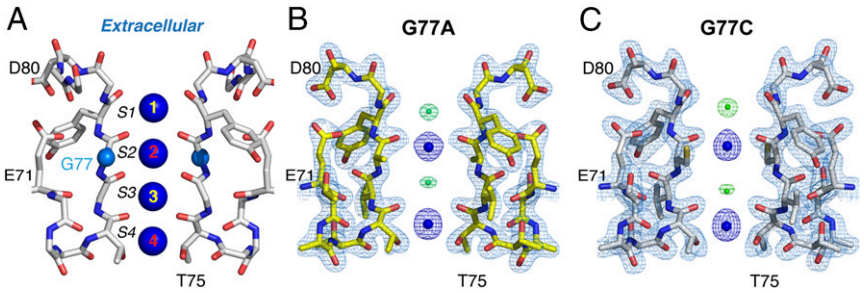

Fig. 1. Structure of the 2,4-ion–bound configuration of a K^+-channel selectivity filter (SF). (*A*) A cartoon representation of KcsA SF, underlining the position of the backbone carbonyl groups from 2 subunits relative to the 4 coordinated K^+ ions. (*B*) G77A structure (PDB is 6NFU) solved at 2.09-Å resolution. A 2Fo-Fc electron-density map (light blue, contoured at 2.3 σ) validating KcsA's SF structural model colored in yellow. Two K^+ ions are bound to the SF (shown as dark-blue spheres), 1 at the S2 site and the other at the S4 site (dark blue, contoured at 3σ). K^+ ions are interspaced with 2 water molecules, 1 coordinated by 8 main-chain carbonyl groups at the S1 site while the other is hydrogen-bonded to the amide nitrogen atoms of Val^{76}. (*C*) Crystal structure of the G77C mutant (PDB is 6NFV) at 2.13 resolution. A 2Fo-Fc electron-density map of the SF is shown in light blue (mesh, contoured at 2.5 σ). The SF is colored in white with the oxygen atoms in red. Two K^+ ions were modeled as blue spheres (dark-blue mesh, contoured at 3.3 σ). As in *B*, 2 water molecules were bound to the channel's SF and modeled as green spheres (at the S1 and S3 sites).

absolute occupancy of thallium ions within KcsA's SF (7) using only anomalous data (15). It was argued then that the absolute ion occupancy of KcsA's SF based on anomalous data (i.e., thallium ions) and of MthK and Kir3.1 based on the native dataset (i.e., potassium ions) was always close to unit occupancy. However, there are several reasons that make this calculation, within a K^+-channel's SF based on electron-density maps, quite problematic and a technical challenge for X-ray crystallography: 1) KcsA SF's binding sites that are not coordinating K^+ ions could be occupied by water molecules, and the electron-density difference between K^+ ions and water molecules is not very large ($18e^-$ [K^+ ions] → $10e^-$ [water molecules] = $8e^-$); 2) the K^+-ions occupancy and their temperature factor (*B*-factor) are related, which creates unavoidable uncertainties in assessing the SF's absolute ion occupancy (15); 3) calculation of ion occupancy derived from anomalous electron-density maps could be incorrect since it relies heavily on the quality of the refined model (7); and 4) the ion occupancy of the S2 and S3 sites is unlikely to be ∼100% since it is drastically reduced by the opening of the activation gate, which in the C-terminal–truncated channel, even at basic pH, happens with a modest probability (Fig. 2*E*) (20, 21). Altogether, all these technical limitations have obviously precluded the precise determination of the K^+ channel's SF absolute ion occupancy by X-ray crystallography, as it has been evidenced by the incongruent values reported for the same K^+ channel by different groups (7, 15, 16). These serious shortcomings of crystallography in the ion-channel research field have led to the proposal of the 2 known highly contrasting mechanisms for ion permeation in K^+ channels (7, 16).

An alternative experimental approach to distinguish between the 2 competing models for ion permeation in K^+ channels is the perturbation of the SF by mutagenesis to eliminate with surgical precision 1 K^+-binding site and then evaluate the functional, thermodynamic, and structural consequences of such insult. This strategy circumvents the aforementioned limitations in the calculation of the SF's absolute ion occupancy and provides structural and energetic invaluable information. It follows that the precise elimination of a single K^+-ion–binding site within KcsA's SF should render an aggregate of 3 K^+ ions in accordance with the direct knock-on mechanism (7), since the model predicts that at 0-mV membrane potential each binding site should be ∼100% occupied. Additionally, it is also predicted by the direct knock-on model that a channel with 3 K^+-ion–binding sites should not be K^+-selective (19). Alternatively, if the highly selective ion permeation displayed by K^+ channels is triggered by the rapid interconversion between 2 isoenergetic ion-bound configurations (1,3 and 2,4) as predicted by the canonical model (16), then the elimination of 1 K^+-binding site should render a channel highly K^+-selective and with an SF stabilized in 1 of the ion-bound configurations.

Results

Crystal Structure of the 2,4-Ion–Bound Configuration of a K^+ Channel. Here, we report a single point mutation within the K^+ channel's SF that stabilizes it in the water–K^+–water–K^+ or 2,4-ion–bound configuration. In this mutant channel, Gly^{77} within the signature sequence of K^+ channels (i.e., TTV**G**YGD) (*SI Appendix*, Fig. S1) was replaced with an Ala or a Cys residue. The structures of the G77A (PDB is 6NFU) and G77C (PDB is 6NFV) mutants were solved by molecular replacement (*SI Appendix*, Table S1). The structural models for these mutant channels were built and refined to a resolution of 2.09 and 2.13 Å, respectively, with R_{work}/R_{free} values of less than 0.24.

The high-quality electron-density maps for either mutant revealed 3 interesting structural differences in their SFs, compared with the KcsA wild-type channel (KcsA-WT). First, mutations at the Gly^{77} prevent the main-chain carbonyl group of Val^{76} from pointing toward the channel's pore, which produces a K^+-ion vacancy at the S3 site. Second, the K^+ ion bound to the S2 site is only coordinated by the 4 main-chain carbonyl groups from the Ala or Cys-77. Third, their SFs showed a striking reduction of the ion occupancy at the S1 site, as if the K^+ ions bound to the S1 and S3 sites were energetically coupled (Fig. 1 *B* and *C*). This structural perturbation yielded a KcsA's SF with K^+ ions bound to the S2 and S4 sites, efficiently stabilizing the 2,4-ion–bound configuration. A structural alignment of the KcsA-WT and the Gly mutant's SF (*SI Appendix*, Fig. S5) indicates a similar overall fold (rmsd ≤ 0.3 Å for the SF atoms) with the only differences being the amino acid side-chain at position 77 and the flipped carbonyl group at Val^{76} (Fig. 1 *B* and *C*). There were 2 positive small electron densities at positions 1 and 3 that were modeled as water molecules (Fig. 1 *B* and *C*).

The interatomic distance between the ions at the S2 and S4 sites for the KcsA-WT, G77A, and G77C were basically identical, ∼6.6, 6.3, and 6.4 Å (*SI Appendix*, Fig. S5), respectively, which supports the idea that these structures represent the 2,4-ion–bound configuration. This experimental result provides concrete evidence that 2 isoenergetic ion-bound configurations coexist within a K^+ channel's SF and that we have isolated the 2,4-ion–bound configuration. It follows that at steady state conditions, the ions bound at the S2 and S4 sites have minimized their electrostatic repulsion by being separated ∼6 Å. This ion-bound arrangement precludes the binding of an ion at the S1 site due to strong electrostatic repulsion with the K^+ ion always

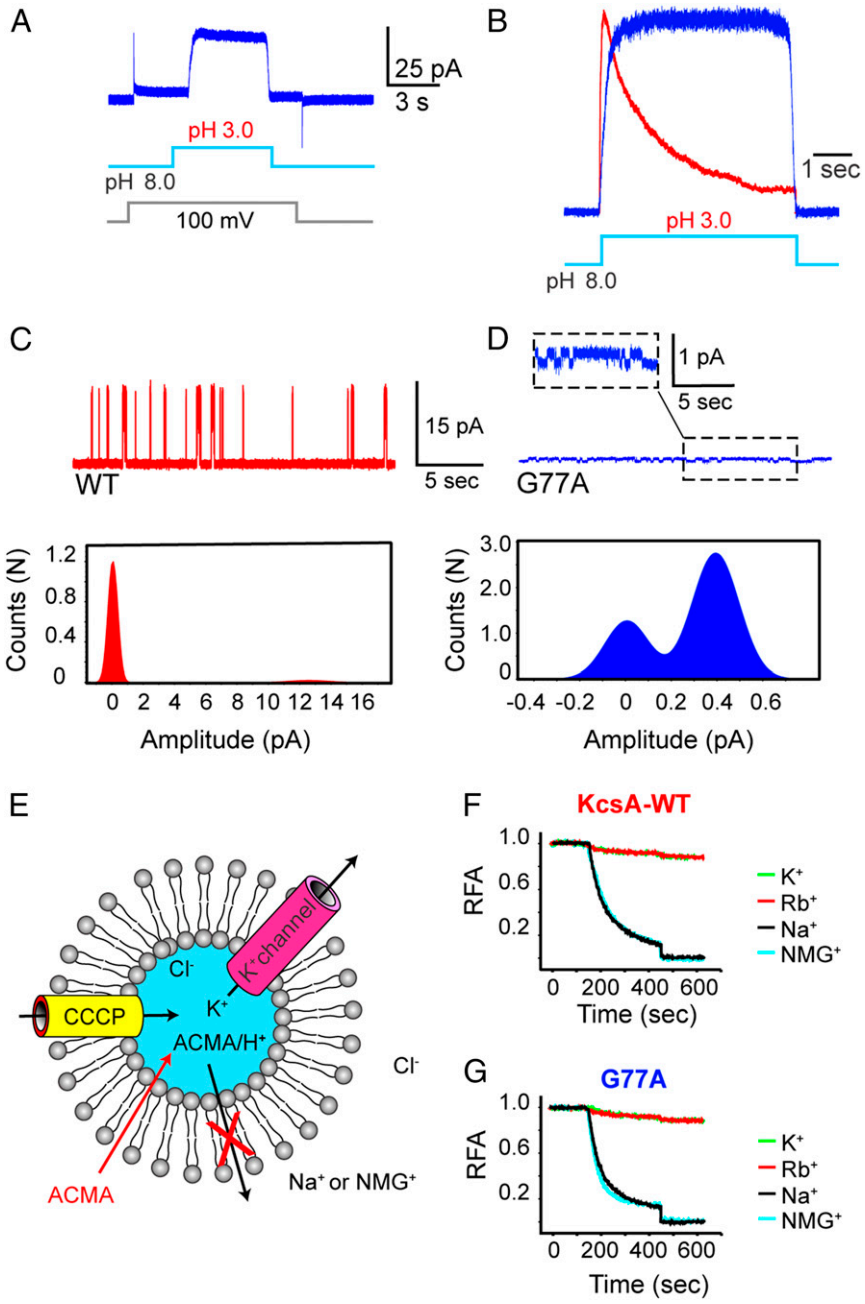

Fig. 2. Functional evaluation of the G77A mutant. (*A*) A macroscopic current recording of the G77A mutant was elicited by a pH jump from 8.0 to 3.0. (*B*) Amplitude-normalized macroscopic currents of the KcsA-WT (red) and the noninactivating G77A mutant (blue). (*C*) A single-channel recording of the KcsA-WT (red) and (*D*) the G77A mutant (blue) measured at 200 mV, 200 mM KCl, alongside their all-point histogram; the chord conductance at 200 mV was ~63 and ~1.95 pS, respectively. (*E*) KcsA-WT- or G77A-containing proteoliposomes preloaded with KCl were diluted in a buffer containing the nonpermeant ions (Na^+ or NMG^+). This generates a large [K^+] difference that favors K^+ efflux. The sequential addition of the fluorescent probe, 9-amino–6-chloro–2-methoxyacridine (ACMA) and the protonophore, carbonyl cyanide m-chlorophenylhydrazone (CCCP) initiates an influx of H^+ that compensates for the K^+ efflux. H^+ uptake is tracked by the ACMA H^+-dependent quenching. (*F*) A robust quenching was observed in the KcsA-WT–containing proteoliposomes, only when diluted in Na^+ or NMG^+ buffer solutions and negligible in a solution containing K^+ or Rb^+ ions. (*G*) The G77A mutant-containing liposomes displayed an ACMA H^+-dependent quenching only when diluted in a Na^+ and NMG^+ solution as did the KcsA-WT. RFA, relative fluorescence of ACMA.

present at the S2 site. Additionally, these 2 KcsA structures are in clear contradiction with the ion-bound configuration predicted by the direct knock-on model for ion permeation in K^+ channels. This model predicts that at steady state conditions, at 0-membrane potential, each of the 4 K^+-binding sites within the K^+ channel's SF should be fully occupied (~100% occupancy). Therefore, the expected ion-bound configuration of the SF, according to the direct knock-on model, of the G77C or G77A mutants must have K^+ ions bound at the S1, S2, and S4 sites since according to this model, these binding sites are independent (they are not coupled), and the perturbation or destruction of a particular binding site should not affect the ion occupancy of the others.

The energetic coupling between the 2 alternating ion-bound configurations of the K^+ channel's SF was also previously inferred from the crystal structure of the KcsA-T75C mutant (22). The S4 site of a K^+ channel's SF is made of 4 carbonyl groups from the

peptide backbone and 4 hydroxyl groups from the side-chain of Threonine 75. The introduction of a cysteine residue at position 75 effectively reduced the number of hydroxyl ligands by 4, producing a significant reduction in the ion occupancy at the S4 site. Concomitantly, the ion occupancy of the S2 site of the T75C mutant was reduced as if the S2 and the S4 sites were energetically coupled.

Altogether, the previously known T75C mutant that favors the 1,3- over the 2,4-ion–bound configuration (22) and our G77A or G77C mutant structures that selectively isolate the 2,4-ion–bound configuration represent the most decisive experimental evidence of the alternating ion-bound configurations within the K^+ channel's SF proposed by the canonical model, and hence they are impossible to reconcile with the proposed direct knock-on model (7).

The stabilization of the water–K^+–water–K^+ configuration by the G77A and G77C mutants provides strong experimental support to the canonical model for ion permeation in K^+ channels. Additionally, this experimental observation validates the coupled transport of water molecules and K^+ ions determined by streaming potential measurements in a Ca^{2+}-activated K^+ channel (23), a K^+ channel of sarcoplasmic reticulum (10), and KcsA (6). However, it is worthwhile to mention that the proponents of the direct knock-on mechanism argued that the streaming potential measurements are not incompatible with their proposed model, since alternated cycles of 4 K^+ and 4 water molecules can explain this phenomenon (19). This idea has a serious caveat in regard to the transport of 4 water molecules per cycle of transport, since in the absence of K^+ ions the SF collapses and adopts a nonconductive conformation (16).

Permeation Properties and Ion Selectivity of the G77A Mutant. We reasoned that the G77A or G77C mutants represent a unique opportunity to assess ion selectivity and ion conduction of a channel with an SF stabilized in the 2,4-ion–bound configuration. We decided to perform a systematic functional characterization of the G77A mutant, given its remarkable stability, structural equivalence with the G77C, and high protein yield.

The G77A mutant conduction properties were evaluated by patch-clamp methods of giant proteoliposomes. Interestingly, the mutant channel when reconstituted at a protein-to-lipid ratio that would normally produce nA-macroscopic current consistently elicited small noninactivating currents, peak amplitude ≤ 100 pA ($n = 20$) in symmetrical 200 mM KCl at pH 3.0 (Fig. 2 *A* and *B*). Puzzled by this experimental result, we actively pursued the G77A single-channel activity by reconstituting the mutant channel at very low protein-to-lipid ratios. Single-channel recordings of the G77A mutant confirmed that its conduction properties were severely affected. The chord conductance at 200 mV was ~1.95 pS ± 0.2 in symmetrical 200 mM KCl, pH 3.0 ($n = 3$) (Fig. 2*D*). This represents a net reduction in the transport rate of about 32 times since KcsA-WT displays a chord conductance at 200 mV of ~63 pS ± 0.4 in the same buffer composition ($n = 3$) (Fig. 2 *C* and *D*). From the all-point histogram it was clearly deduced that the G77A mutants displayed a higher open probability, which is explained by the elimination of C-type inactivation exhibited by this mutant (Fig. 2*B*). Such a dramatic reduction in unitary conductance has been previously reported for other KcsA mutants, in which the ion occupancy of the SF-binding sites has been markedly reduced. The T75C mutant that reduced the ion occupancy at the S4 and S2 sites displayed ~25-pS single-channel conductance (22); the T75A mutant exhibited a more pronounced reduction in unitary conductance, ~7 pS (24).

The distinct reduction in single-channel conductance shown by the G77A mutant was predicted on computational grounds in a very elegant quantum mechanical study. This study proposes that the strength of the ligating oxygens, the "tunability" of the environment surrounding the ion-binding site (phase activation), and the coordination number are the key elements to produce very efficient ion-selective partitioning of the K^+ ions from the aqueous phase into the SF's binding sites (25, 26). It follows that the G77A mutant, by lacking the 4 ligating oxygens located between the S2 and the S3 sites, the 2 less–water-exposed binding sites (Fig. 1), effectively perturbs the ion coordination number at 2 consecutive binding sites. This structural perturbation, as predicted by Varma et al. (26), will introduce a very large electrostatic penalty when transferring an ion from the environment into to the SF's binding sites, which in turn reduces the free energy for K^+-ion partitioning into the filter, and as a consequence these mutants presented a drastically reduced single-channel conductance. Although this structural perturbation drastically reduced the channel's transport rate, it does represent a unique tool to separate ion binding from the permeation process.

To study the G77A ion selectivity, we used a well-established fluorescent-based K^+ flux assay given its reduced single-channel conductance (27). Briefly, C-terminal–truncated KcsA-containing proteoliposomes preloaded with 200 mM KCl (the truncated version displays a higher channel activity at neutral pH) were diluted into a buffer containing 200 mM of nonpermeant ions (i.e., Na^+ or NMG^+). The large K^+ concentration difference between the inside and the outside of the proteoliposomes drives the selective exit of K^+ ions via KcsA, which in turn produces a membrane electrical potential (negative inside). Next, upon the sequential addition of the membrane-permeable pH-sensitive ACMA dye and the protonophore CCCP, a clear time-dependent quenching by protons of the ACMA fluorescence was observed, (i.e., protons will enter via CCCP only if KcsA is active and K^+-selective) (Fig. 2 *E* and *F*). On the contrary, if KcsA-containing liposomes are diluted in a buffer with 200 mM of K^+ or Rb^+, no membrane potential can be established, and hence no quenching of the ACMA fluorescence was observed (Fig. 2*F*). Interestingly, when K^+-loaded liposomes containing the C-terminal–truncated G77A mutant were diluted in a buffer having an equal concentration of Na^+ or NMG^+, a KcsA-WT–like time-dependent quenching of ACMA fluorescence was observed (Fig. 2*G*). These results demonstrated that contrary to what is known for the *Shaker* channel (5), mutations at the Gly^{77} (TTV**G**YGD) yielded a channel with a well-preserved selectivity for K^+ over Na^+ or NMG^+ ions.

Interestingly, although the G77A mutant displayed a marked reduction in single-channel conductance, as a consequence of the reduction in the number of the ligating carbonyl groups, the mutant channel remained as K^+-selective as the wild-type KcsA. This experimental result is quite interesting and hints at the high complexity of the ion-selective partitioning mechanism displayed by the SF of K^+ channels. Computational studies and experimental evidence have suggested that a reduction in the number of ligating carbonyl groups (26, 28), reduction in the number of ion-binding sites (less than 4) (3), and/or the presence of intervening water-filled cavities (29, 30) effectively eliminates the high K^+ over Na^+ ion selectivity displayed by K^+ channels. However, the G77A mutant, despite presenting a reduction in the number of the ligating carbonyl groups and in the number of ion-binding sites, remained wild-type–like ion-selective. These experimental findings are in agreement with a recent report, in which an alanine substitution at the highly conserved Threonine residue within the signature sequence on K^+ channels, i.e., TTVGYGD, of the bacterial KcsA, the fruit fly *Shaker*, and the human Kv1.5 channels did not affect their characteristic high K^+ over Na^+-ion selectivity despite markedly reducing the number of ligating oxygen atoms at the S4 site and, as a consequence, reducing the number of K^+-binding sites within the channel's SF (24).

Conflictingly, a recent molecular dynamic simulation study indicated that the characteristic high ion selectivity displayed by K^+ channels is only possible when water extrusion and full occupancy of the 4 ion-binding sites within the K^+ channel's SF are achieved as is predicted by the direct knock-on mechanism (19).

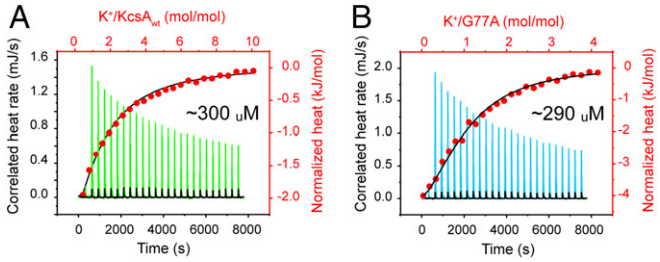

Fig. 3. Ion-binding properties of the 2–4 ion bound configuration of a K^+-channel selectivity filter. An isothermal titration calorimetry (ITC) experiment in which (*A*) KcsA-WT or (*B*) the G77A (previously dialyzed against 50 mM Tris-Cl, pH 8.0, 100 mM NaCl, and 5 mM Dodecyl Maltoside) were titrated with a 5 mM KCl solution at 25 °C. Approximately 380 μM KcsA-WT or the G77A samples were placed in the Nano ITC microcalorimeter sample cell. An upward peak corresponds to 1 injection (green trace). A 5-mM KCl solution was titrated into the dialysis buffer in the absence of protein as the buffer control, and the heat change associated with dilution was subtracted from the thermogram (black trace). The area under each peak represents the heat exchange. The normalized heat changes (kJ/mol) for the KcsA-WT (*A*) or the G77A (*B*) were plotted versus their respective molar ratios (red dots) and fitted with an independent binding model assuming a fixed stoichiometry, $n = 1$ (black line). The apparent K^+ dissociation constants (K_d) for the KcsA-WT 0.3 ± 0.04 mM, shown in *A*, and the G77A mutant 0.29 ± 0.02 mM, shown in *B*, are the average of 5 ($n = 5$) independent determinations.

The structure of the KcsA G77C and G77A mutants clearly contradict this prediction since their SFs are missing the S3 site, they display low ion occupancy at the S1 site, and they clearly contain intervening water molecules between their K^+-ion–binding sites; yet they are as K^+-selective as the KcsA wild-type channel. These experimental observations clearly and decisively indicate that neither water extrusion nor full-ion occupancy, as was recently proposed based on the direct knock-on mechanism (19), are essential for the characteristic high K^+-over Na^+-ion selectivity displayed by the superfamily of K^+-selective channels.

Thus, it seems that the G77A mutation isolates the initial steps involving K^+ binding to the channel's SF from the permeation process as has been done from a theoretical perspective in very elegant computational works (26). Hence, it represents a unique opportunity to assess the thermodynamics of K^+ binding to a K^+ channel's SF stabilized in the 2,4-ion–bound configuration.

Ion-Binding Properties of the 2,4-Ion–Bound Configuration of a K^+ Channel's SF. The apparent K^+-binding affinity for the KcsA's SF under equilibrium conditions was measured by isothermal titration calorimetry (ITC), as has been done before for measuring the apparent cation-binding affinity to membrane transporters (31, 32). This measurement is considered an apparent ion-binding affinity because it was performed in the presence of 100-mM Na^+ ions, which could compete against K^+ ions for the SF's ion-binding sites. The absolute K^+-binding affinity can be assessed in the total absence of Na^+ ions, but in such experimental conditions, KcsA at such high protein concentration displayed marked precipitation, which precluded the realization of these types of affinity measurements. Therefore, the apparent dissociation constant (K_d) of K^+ ions binding to the KcsA-WT and the G77A channel's SF in the presence of 100 mM Na^+ were virtually identical, 0.30 ± 0.04 mM and 0.29 ± 0.02 mM ($n = 5$), respectively (Fig. 3 *A* and *B*). Outstandingly, these K^+-binding measurements (carried out in the presence of 100 mM NaCl) indicated that the characteristic high K^+- over Na^+-ion–binding selectivity was fully preserved in the G77A mutant; otherwise the G77A would not discriminate between the 2 monovalent ions used in our experimental conditions.

It follows that either of the 2 G77A-SF ion-binding sites, S2, S4, or both (Fig. 1 *B* and *C*), is/are the titratable site(s) assessed by our ITC experiments. Interestingly, the best mathematical fitting of the ITC data was achieved assuming $n = 1$ or 1 binding site. To determine the G77A-titratable ion-binding site(s), we solved the structure of the G77A mutant in 300 mM NaCl by macromolecular crystallography. Crystals diffracted X-rays to 2.05-Å resolution, and the structure was solved by molecular replacement ($R_{work} = 0.198$ and $R_{free} = 0.235$). The G77A's SF structure in Na^+ ions clearly showed a marked reduction of the ion occupancy at the S2 site, which demonstrates that under our experimental conditions this is the titratable ion-binding site within the G77A's SF or the 2,4-ion–bound configuration. Consequently, the apparent dissociation constant measured by isothermal titration calorimetry more likely corresponds to the binding of K^+ ions to the S2 site (Fig. 4). In support of this idea, a positive electron-density at the S4 site was modeled as an Na^+ ion (based on the number of observed ligating oxygens, O = 4), which was coordinated exclusively by the side-chain carboxyl group from Thr^{75}. The G77A's SF structure in 300-mM Na^+ ions explains why the ITC data were best fit assuming $n = 1$; there is only 1 K^+-selective binding site within the 2,4-ion–bound configuration of a K^+-channel's SF. The fact that the S4 site can coordinate K^+ and Na^+ ions speaks of its true non–K^+-selective nature. The latter statement is in total agreement with previous mutagenesis studies, in which the S4 site was perturbed and its ion occupancy drastically reduced by changing the Thr^{75} to a cysteine or an alanine residue in several representative members of the K^+-selective channel family, yet the mutant channels remained wild-type–like K^+-selective (22, 24).

Finally, a very elegant computational study has previously suggested that the KcsA S2 site is the most K^+-selective binding site of the channel's SF, which we have now proved experimentally (12).

Discussion

Locally, the alanine residue at position 77 effectively precludes the SF structural changes associated with K^+-ion depletion or

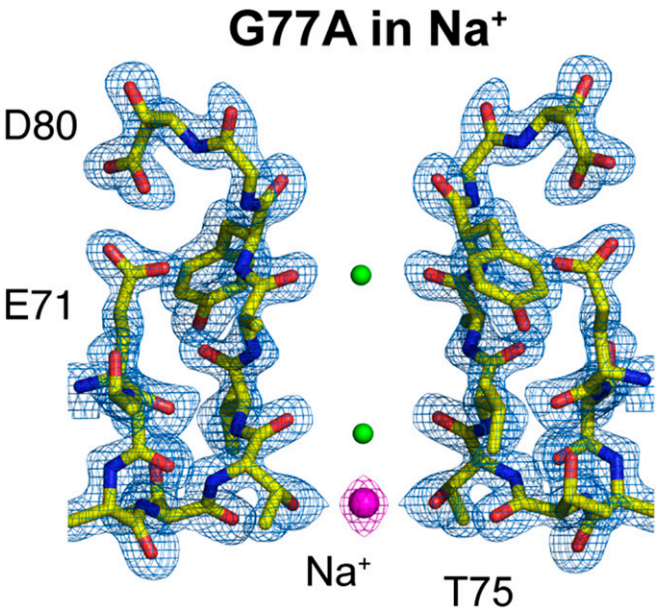

Fig. 4. Crystal structure of the G77A mutant in 300 mM sodium chloride. The G77A structure solved in the presence of 300 mM NaCl at 2.05-Å resolution (PDB is 6PA0). A 2Fo-Fc electron-density map (light blue, contoured at 2.6 σ) validates the SF structural model colored in yellow. One Na^+ ion is bound to the S4 site by the carboxyl group of Thr^{75} (presented as magenta spheres). Two small positive electron densities were modeled as water molecules (represented as small green spheres).

C-type inactivation gating, which are typical structural changes of the wild-type KcsA's SF (16, 20, 33).

Altogether, our experimental results provide strong and tangible evidence of the original proposed alternating K^+-ion–bound configurations within KcsA channel's SF, the archetypal K^+-channel pore domain (15, 18). The G77A mutation, by selectively vacating the S3 site, also drastically reduced the ion occupancy of the S1 site and in steady state conditions displayed ions bound only at the S2 and S4 sites, which is an experimental result that cannot be explained by or reconciled with the direct knock-on model that predicts an aggregate of 3 K^+ ions bound to the G77A or G77C SF structures. Additionally, the high K^+ over Na^+ ion selectivity shown by the G77A mutant channel is in total contradiction and cannot be reconciled with the idea that only a channel with an SF with 4 contiguous bound K^+ ions, as is predicted by the direct knock-on model, can be highly K^+-selective.

Hence, we are proposing that G77A SF favors the 2,4-ion–bound configuration, and thus the concurrent occupancy of the S1- and S2-binding sites is energetically improbable due to a very strong electrostatic repulsion. Additionally, the finding that the stabilized 2,4-ion–bound configuration binds K^+ ions with the same apparent binding affinity as it does the KcsA-WT allows us to propose that the alternating 1,3-ion–bound configuration likely has the same affinity for K^+ ions, which underscores the original proposal of 2 isoenergetic ion-bound configurations coexisting within the potassium-channel SF (16).

Materials and Methods

KcsA-WT, G77A, and G77C were expressed and purified as described before (34). C-terminal–truncated KcsA (wild-type, G77A, and G77C) was mixed with an antibody fragment needed for the crystallization process. The channel-Fab complex was purified by passing it through a size-exclusion chromatography column, ENrich SEC 650 10 × 300 column (Bio-Rad) preloaded with Buffer TKS (Buffer TKS: 50 mM Tris·HCl: 150 mM KCl, pH 8.0) + 0.5 mM Dodecyl Maltoside (the G77A or G77C channels did not crystallize in the commonly used decyl maltoside detergent; instead a systematic search was conducted to determine the optimal conditions for crystallization). Crystal trials were performed by the sitting-drop method in 22 to 26% PEG400 (vol/vol), 50 mM magnesium acetate, 50 mM sodium acetate (pH 4.8. to 5.4). A dataset was acquired from a single crystal for the G77A or the G77A mutants at the Beamline 14-1 at the Stanford Synchrotron Radiation Laboratory (SSRL). Image processing and data reduction were performed with HKL2000 (35). Electrophysiological recordings: KcsA-G77A mutant or KcsA wild-type channels were reconstituted in Asolectin liposomes as described before (36). ITC determinations were conducted in a Nano Isothermal Titration Calorimeter (TA Instruments) at 25 °C. The protein sample (~380 μM KcsA WT or G77A) was placed in a sample cell that contained a reaction volume of ~170 μL. The KCl solutions used to titrate the dialyzed KcsA sample were prepared in the dialysis buffer used during the last dialysis step, and they were degassed for 30 min prior to starting the titration experiments using a TA Instruments degassing instrument (model 63256). To assess the ion selectivity of KcsA-WT and the G77A mutant a fluorescent liposome flux assay that has been used before to evaluate the function of ion channels was adapted for this purpose (37). Additional details are described in *SI Appendix*.

ACKNOWLEDGMENTS. We thank Dr. Luis Reuss, Dr. Guillermo Altenberg, and Dr. Alain Labro for insightful discussions and comments during the data analysis and interpretation of this project. We thank Silvia Russi at the SSRL Beamline 14-1 for assistance at the synchrotron. This work was supported by NIH Award 2R01GM097159-06 and Welch Foundation Award (BI-1949) (to L.G.C.), as well as NIH Awards R01GM122759 and R21NS105863 (to L.G.).

1. J. Aqvist, V. Luzhkov, Ion permeation mechanism of the potassium channel. *Nature* **404**, 881–884 (2000).
2. S. Bernèche, B. Roux, A gate in the selectivity filter of potassium channels. *Structure* **13**, 591–600 (2005).
3. M. G. Derebe *et al*., Tuning the ion selectivity of tetrameric cation channels by changing the number of ion binding sites. *Proc. Natl. Acad. Sci. U.S.A.* **108**, 598–602 (2011).
4. S. Furini, C. Domene, Atypical mechanism of conduction in potassium channels. *Proc. Natl. Acad. Sci. U.S.A.* **106**, 16074–16077 (2009).
5. L. Heginbotham, Z. Lu, T. Abramson, R. MacKinnon, Mutations in the K+ channel signature sequence. *Biophys. J.* **66**, 1061–1067 (1994).
6. M. Iwamoto, S. Oiki, Counting ion and water molecules in a streaming file through the open-filter structure of the K channel. *J. Neurosci.* **31**, 12180–12188 (2011).
7. D. A. Kopfer *et al*., Ion permeation in K(+) channels occurs by direct coulomb knock-on. *Science* **346**, 352–355 (2014).
8. H. T. Kratochvil *et al*., Instantaneous ion configurations in the K+ ion channel selectivity filter revealed by 2D IR spectroscopy. *Science* **353**, 1040–1044 (2016).
9. H. T. Kratochvil *et al*., Probing the effects of gating on the ion occupancy of the K^+ channel selectivity filter using two-dimensional infrared spectroscopy. *J. Am. Chem. Soc.* **139**, 8837–8845 (2017).
10. C. Miller, Coupling of water and ion fluxes in a K+-selective channel of sarcoplasmic reticulum. *Biophys. J.* **38**, 227–230 (1982).
11. J. H. Morais-Cabral, Y. Zhou, R. MacKinnon, Energetic optimization of ion conduction rate by the K+ selectivity filter. *Nature* **414**, 37–42 (2001).
12. S. Y. Noskov, S. Bernèche, B. Roux, Control of ion selectivity in potassium channels by electrostatic and dynamic properties of carbonyl ligands. *Nature* **431**, 830–834 (2004).
13. F. I. Valiyaveetil, M. Leonetti, T. W. Muir, R. Mackinnon, Ion selectivity in a semisynthetic K+ channel locked in the conductive conformation. *Science* **314**, 1004–1007 (2006).
14. J. Zheng, F. J. Sigworth, Intermediate conductances during deactivation of heteromultimeric Shaker potassium channels. *J. Gen. Physiol.* **112**, 457–474 (1998).
15. Y. Zhou, R. MacKinnon, The occupancy of ions in the K+ selectivity filter: Charge balance and coupling of ion binding to a protein conformational change underlie high conduction rates. *J. Mol. Biol.* **333**, 965–975 (2003).
16. Y. Zhou, J. H. Morais-Cabral, A. Kaufman, R. MacKinnon, Chemistry of ion coordination and hydration revealed by a K+ channel-Fab complex at 2.0 A resolution. *Nature* **414**, 43–48 (2001).
17. A. L. Hodgkin, R. D. Keynes, The potassium permeability of a giant nerve fibre. *J. Physiol.* **128**, 61–88 (1955).
18. M. Zhou, J. H. Morais-Cabral, S. Mann, R. MacKinnon, Potassium channel receptor site for the inactivation gate and quaternary amine inhibitors. *Nature* **411**, 657–661 (2001).
19. W. Kopec *et al*., Direct knock-on of desolvated ions governs strict ion selectivity in K^+ channels. *Nat. Chem.* **10**, 813–820 (2018).
20. L. G. Cuello, V. Jogini, D. M. Cortes, E. Perozo, Structural mechanism of C-type inactivation in K(+) channels. *Nature* **466**, 203–208 (2010).
21. L. G. Cuello, D. M. Cortes, V. Jogini, A. Sompornpisut, E. Perozo, A molecular mechanism for proton-dependent gating in KcsA. *FEBS Lett.* **584**, 1126–1132 (2010).
22. M. Zhou, R. MacKinnon, A mutant KcsA K(+) channel with altered conduction properties and selectivity filter ion distribution. *J. Mol. Biol.* **338**, 839–846 (2004).
23. C. Alcayaga, X. Cecchi, O. Alvarez, R. Latorre, Streaming potential measurements in Ca2+-activated K+ channels from skeletal and smooth muscle. Coupling of ion and water fluxes. *Biophys. J.* **55**, 367–371 (1989).
24. A. J. Labro, D. M. Cortes, C. Tilegenova, L. G. Cuello, Inverted allosteric coupling between activation and inactivation gates in K^+ channels. *Proc. Natl. Acad. Sci. U.S.A.* **115**, 5426–5431 (2018).
25. S. Varma, S. B. Rempe, Coordination numbers of alkali metal ions in aqueous solutions. *Biophys. Chem.* **124**, 192–199 (2006).
26. S. Varma, D. M. Rogers, L. R. Pratt, S. B. Rempe, Perspectives on: Ion selectivity: Design principles for K+ selectivity in membrane transport. *J. Gen. Physiol.* **137**, 479–488 (2011).
27. Z. Su, E. C. Brown, W. Wang, R. MacKinnon, Novel cell-free high-throughput screening method for pharmacological tools targeting K+ channels. *Proc. Natl. Acad. Sci. U.S.A.* **113**, 5748–5753 (2016).
28. S. Varma, S. B. Rempe, Tuning ion coordination architectures to enable selective partitioning. *Biophys. J.* **93**, 1093–1099 (2007).
29. S. Y. Noskov, B. Roux, Importance of hydration and dynamics on the selectivity of the KcsA and NaK channels. *J. Gen. Physiol.* **129**, 135–143 (2007).
30. N. Shi, S. Ye, A. Alam, L. Chen, Y. Jiang, Atomic structure of a Na+- and K+-conducting channel. *Nature* **440**, 570–574 (2006).
31. S. W. Lockless, M. Zhou, R. MacKinnon, Structural and thermodynamic properties of selective ion binding in a K+ channel. *PLoS Biol.* **5**, e121 (2007).
32. P. Hariharan, L. Guan, Thermodynamic cooperativity of cosubstrate binding and cation selectivity of *Salmonella typhimurium* MelB. *J. Gen. Physiol.* **149**, 1029–1039 (2017).
33. L. G. Cuello, D. M. Cortes, E. Perozo, The gating cycle of a K^+ channel at atomic resolution. *eLife* **6**, e28032 (2017).
34. C. Tilegenova, S. Vemulapally, D. M. Cortes, L. G. Cuello, An improved method for the cost-effective expression and purification of large quantities of KcsA. *Protein Expr. Purif.* **127**, 53–60 (2016).
35. Z. Otwinowski, W. Minor, Processing of X-ray diffraction data collected in oscillation mode. *Methods Enzymol.* **276**, 307–326 (1997).
36. D. M. Cortes, L. G. Cuello, E. Perozo, Molecular architecture of full-length KcsA: Role of cytoplasmic domains in ion permeation and activation gating. *J. Gen. Physiol.* **117**, 165–180 (2001).
37. J. R. Whicher, R. MacKinnon, Structure of the voltage-gated K(+) channel Eag1 reveals an alternative voltage sensing mechanism. *Science* **353**, 664–669 (2016).